BGS candidate models for IGRF-13

Team institution: British Geological Survey
Team members: William Brown (wb@bgs.ac.uk)
Ciarán Beggan
Grace Cox
Susan Macmillan

Candidate models submitted:
1. Main field at 2020.0
2. Secular variation for 2020.0—2025.0
3. Main field at 2015.0

1. Data sources and selection

Two data sources were used to construct our candidate models: (1) the ESA Swarm mission and (2) the ground observatory network.

1.1 Ground observatories

Hourly mean vector data were collected from the World Data Centre for Geomagnetism, Edinburgh for the period 2013/01/01 to 2019/07/31. These were supplemented with other more recent data reported to INTERMAGNET, or internally at BGS.

1.2 Swarm

The latest available Swarm data files, up to version 0507, were collected for Alpha, Bravo and Charlie, from the mission start on 2013/11/25 to 2019/08/14.

1.3 Data selection criteria

The following selection criteria were applied to Swarm and observatory data, as summarised Table 1.

Swarm data were subsampled (every 20th datum), and at low geomagnetic dipole (GMD) latitudes were retained only for magnetically quiet, local night times. At high GMD latitudes, no local time selection was used, and an additional filter for the merging electric field was applied. We use vector data at all latitudes. Scalar data from the ASM instruments on Swarm were used only when vector data from the VFM instruments were unavailable. Solar wind parameters were provided by the OMNI2 data set, which includes a forward projection of measurements made at the L1 Lagrange point to Earth's magnetopause.

We also use full field observatory data from 164 locations, at hourly mean cadence, and selected for local night times at all latitudes. Vector data were used below GMD latitude |55°|. Above this latitude, vector data were used to calculate a projection of scalar data onto a prior BGS core field model. The projection of scalar data onto a prior model (pseudo-scalar data) allows a linear relation between the modelled Gauss coefficients and the crustal biases that are required for the solution with full field observatory data.

Table 1: Summary of data selection criteria for Swarm and ground observatory data.

Filter	Description	Satellite	Observatory
Sampling		Every 20th datum	Hourly mean
Kp, Kp_{-3h}	3 hour planetary K index at datum and in preceding 3 hour interval	$\leq 2_0$, $\leq 2_0$	$\leq 2_+$
$\lvert D_{st}\rvert$ [nT], $\lvert dD_{st}/dt\rvert$ [nT/h]	Storm time disturbance and its rate of change per hour at datum	≤30, ≤2	–, ≤5
IMF B_x, B_y, B_z [nT]	Projected Interplanetary Magnetic Field at datum	$\leq\lvert 10\rvert$, $\leq\lvert 3\rvert$, $0\leq x\leq 6$	–, –, ≥-2
v_{sw} [km/s]	Projected solar wind velocity at datum	≤450	–
LT (<|55°GMD|)	Local time at GMD latitudes below |55°|	23:00≤x≤05:00	01:00≤x≤02:00
$\lvert d\text{-}m_{prior}\rvert$ [nT]	Absolute difference between datum and a prior BGS field model estimation	≤100	–
$\lvert F\text{-}\lvert B\rvert\rvert$ [nT]	Absolute difference between ASM and magnitude of VFM data	≤2	–
E_{min} (>|55°GMD|) [mV/m]	Hourly mean of 1 minute merging electric field, calculated as in Olsen *et al*. [2014].	≤0.8	–

The resulting distribution of data in time is shown in Figure 1. The separation of observatories between those providing vector data and those providing projected-scalar data is shown in Figure 2. A total of 5,924,486 data were used.

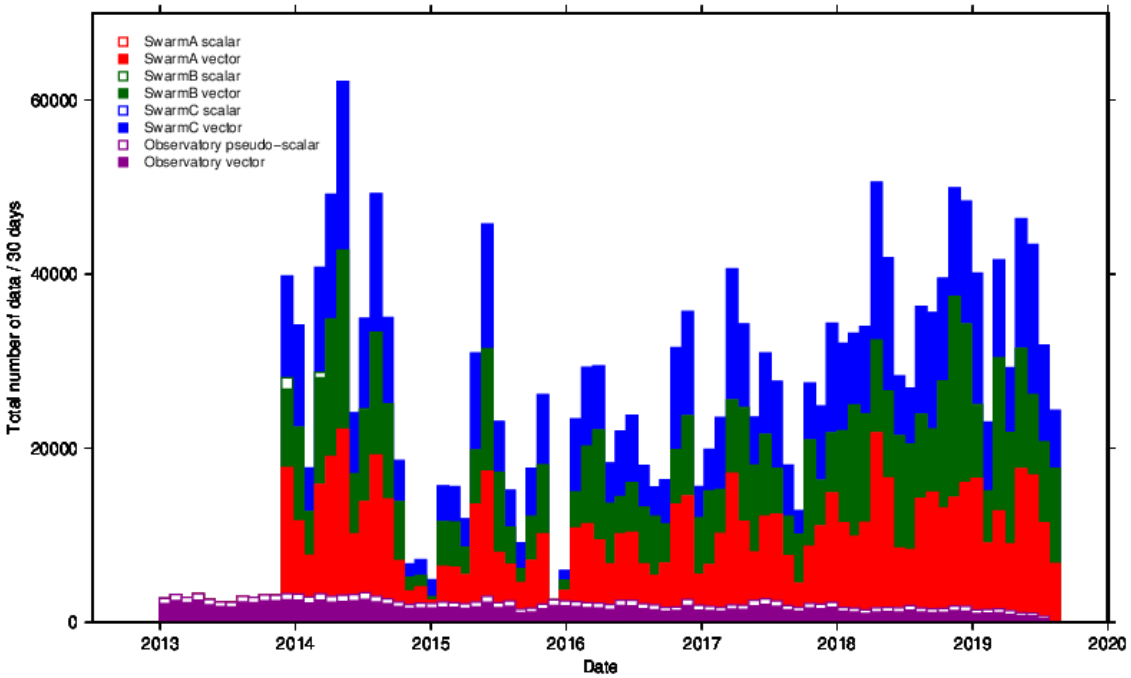

Figure 1: Stacked histogram of data coverage in time, binned each 30 days. Solid bars show vector data, hollow bars show scalar data.

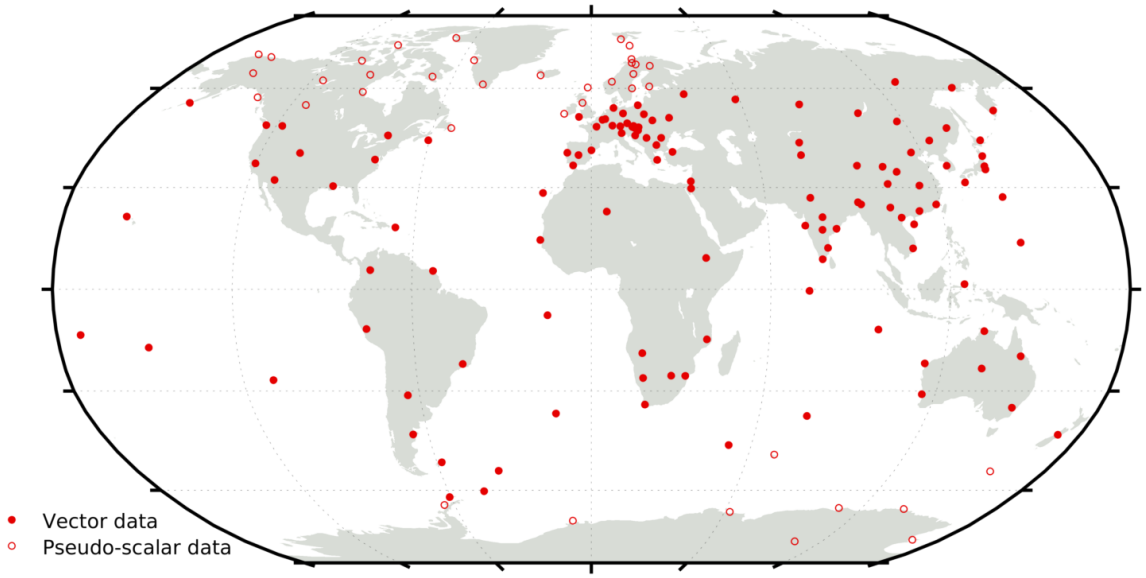

Figure 2: Map of the 164 observatory locations providing hourly data. Closed circles for the 123 locations that provide vector data, open circles for the 41 locations above GMD latitudes |55°| that provide projected scalar data.

2. Data weighting

2.1 Swarm

Satellite data variances were calculated from a combination of noise terms based on:

- Along-track standard deviation calculated over each 20 s segment of 1 Hz data, in each vector component, and for the scalar field.
- External field activity as measured at the geographically nearest magnetic observatories, described by the LAVA index [Thomson *et al.*, 2010]
- Spatially uniform noise (2 nT standard deviation)

- A function of solar zenith angle, *z*, (in nT), $(1 + \cos(z))^2$

These variances were then scaled by data density within 1° equal-area tesserae, such that the dense high latitude data are down weighted.

2.2 Ground observatories

Ground observatory data were given a simpler prior variance:

- Spatially uniform noise for vector data below |55°| GMD latitude (2 nT standard deviation)
- Spatially uniform noise for projected scalar data above |55°| GMD latitude (6 nT standard deviation)
- A function of solar zenith angle, *z*, (in nT), $(1 + \cos(z))^2$

These variances were then scaled by data density within 5° equal-area tesserae, to account for regions such as Europe with very dense coverage. A final scaling factor was applied to the variances of all observatory data such that the total weight is roughly 10% that of the total weight of all satellite data.

3. MEME parent model methodology

The BGS IGRF-13 candidate models are derived from the BGS Model of Earth's Magnetic Environment (MEME) parent model. This MEME co-estimates several field sources simultaneously as described below. The methodology broadly follows that of our IGRF-12 candidate, described by Hamilton *et al.* [2015]. All data and model parameterisations are in the NEC coordinate frame, unless otherwise specified.

Core field:

- spherical harmonic degree and order 15
- order 6 B-spline time dependence
- 6 month spaced knots from 2012.9 to 2019.9
- regularised time integral of the 3rd time derivative of the radial magnetic field over the core-mantle boundary
- regularised 2nd time derivative of the radial magnetic field over the core-mantle boundary at the end knots
- 4845 parameters

Crustal field:

- static in time, described from degrees 16 to 55
- 2880 parameters

Large-scale slowly varying external field:

- spherical harmonic degree and order 1
- order 2 B-spline time dependence
- 3 month spaced knots from 2012.9 to 2019.9
- 87 parameters

Large-scale rapidly varying external and induced field:

- spherical harmonic degree and order 1
- order 2 B-spline time dependence governed by the VMD index [Thomson & Lesur, 2007], with 3 month knots

- 174 parameters

Periodic variations:

- sine and cosine terms accounting for external and induced annual and semi-annual variations, 14 parameters
- external sine and cosine terms accounting for diurnal variations, parameterised by sun-synchronous longitude, 42 parameters

Crustal biases:

- static offsets for each vector component or the scalar at each observatory location to account for unresolved local crustal fields captured in the full field data
- 410 parameters

The model inversion solves for 8452 parameters from 5,924,486 data by least squares regularised minimum norm, using a null starting model and an L2 norm. This was followed by a single iteration of regularised iteratively reweighted least squares, using Huber reweighting and an L2 norm. The initial least squares solution was not significantly altered by the iterative reweighting step and further iterations were similarly shown to be oscillations about the fit minima. Regularisation is applied only to the time varying core field, and is governed by three damping parameters that control the damping at each model end knot, and the time integral, respectively. As our scalar data are projected onto a prior BGS core field model, derived in a similar manner, it is linearly related to our model coefficients.

The final model fit has an overall formal standard deviation of 1.86 nT, a summary of weighted mean and root-mean-square residual misfit is given in Table 2.

Table 2: Number of data by type, and the mean and root-mean-square misfits between model and data, weighted by the inverse of the data variances. Satellite data with subscript 'L' indicate data at GMD latitudes below |55°|, values with subscript 'H' indicate data at GMD latitudes above |55°|. Observatory vector and projected scalar data are only used in the regions below and above |55°| GMD latitude, respectively. Residuals are in NEC coordinates.

			Mean [nT]				RMS [nT]			
	# vector	# scalar	B_N	B_E	B_C	F	B_N	B_E	B_C	F
All Swarm	1,827,440	2,907	0.16	-0.01	-0.07	-2.76	7.90	6.02	4.30	5.76
All Swarm$_L$	569,641	447	0.08	-0.04	-0.10	-2.64	5.85	3.90	2.34	4.08
All Swarm$_H$	1,257,799	2,460	0.69	0.20	0.07	-3.99	15.71	14.39	8.86	14.59
Obs.	130,571	47,546	0.02	0.00	0.00	-0.08	4.86	3.91	3.56	23.33
SwarmA$_L$	190,241	90	0.15	-0.34	-0.14	-0.56	5.59	3.61	2.32	1.88
SwarmA$_H$	419,651	478	0.70	0.21	0.05	-3.18	15.62	14.39	9.05	8.00
SwarmB$_L$	190,899	331	-0.11	0.01	-0.01	-3.62	6.18	4.37	2.31	4.14
SwarmB$_H$	419,743	1,900	0.66	0.21	0.12	-4.19	15.83	14.50	8.53	16.15
SwarmC$_L$	188,501	26	0.19	0.22	-0.17	2.29	5.74	3.62	2.38	0.78
SwarmC$_H$	418,405	82	0.72	0.19	0.03	-5.82	15.69	14.28	9.00	13.42

4. Derivation of IGRF candidate models

The three BGS candidate models were derived from MEME in the following manner. No uncertainties are provided with any of our candidate models.

4.1 Main field at 2015.0

The main field at 2015.0 was taken directly from the core component of MEME, truncating to degree 13.

4.2 Main field at 2020.0

The main field at 2020.0 was extrapolated from the core component of MEME, then truncated to degree 13. The main field of the MEME core component at 2019.0 was used as a datum, to which we added the mean annual core secular variation for the period 2018.25 to 2019.25, sampled at eleven equally spaced time increments, inclusive of the end times.

4.3 Secular variation for 2020.0—2025.0

We use the steady core flow and acceleration formalism as given in Whaler & Beggan [2015] to estimate the 'average' flow and acceleration over 2017.5 to 2019.0. We then forward propagate the estimated main field coefficients of the BGS IGRF2020 candidate from 2020.0 to 2025.0. We compute the difference between 2025.0 and 2020.0 and divide by five to produce the annual SV coefficients for our candidate model (up to degree and order 13) which can be truncated at degree 8 as required.

In detail, we use the monthly SV and SA magnetic field values of the MEME parent model output from 2017.5 to 2019.0 to compute the steady core flow and steady core acceleration over this 1.5-year period. The core flows were computed using an L1-norm iterative-reweighting scheme to fit the flow and acceleration to the SV and SA coefficients (up to degree and order 14 and 8, respectively). We apply also a tangentially geostrophic constraint to the L1-norm solution (see Beggan & Whaler [2008]) before solving for the steady flow and acceleration. Both toroidal and poloidal flow and acceleration are solved for simultaneously. The outputs consist of a steady flow model and steady acceleration model for the period covering 2017.5 to 2019.0.

The forecast from 2020.0 to 2025.0 was made using monthly time-steps (one-twelfth of a year). At each time-step, the Gaunt and Elsasser matrices are computed using the main field model and secular variation from the preceding month. The SV and SA are computed from the Gaunt-Elsasser matrix multiplied by the steady flow and acceleration model and added to the main field to step forward by a month.

The process is repeated from 2020.0 to 2025.0. The main field coefficients for 2020 are subtracted from main field coefficients of 2025.0 to compute the field change over five years. The annual SV is computed by dividing the difference by 5.

5. References

Beggan, C., K. Whaler (2008), Core flow modelling assumptions, *Physics of the Earth and Planetary Interiors*, 167, 217-222. doi: 10.1016/j.pepi.2008.04.011.

Hamilton, B., V. A. Ridley, C. D. Beggan and S. Macmillan (2015), The BGS magnetic field candidate models for the 12th generation IGRF, *Earth, Planets and Space*, 67, doi: 10.1186/s40623-015-0227-x.

Olsen, N., H. Lühr C. C. Finlay, T. J. Sabaka, I. Michaelis, J. Rauberg and L. Tøffner-Clausen (2014), The CHAOS-4 geomagnetic field model. *Geophysical Journal International*, 197(2), 815-827, doi: 10.1093/gji/ggu033.

Thomson, A. W. P., B. Hamilton, S. Macmillan and S. J. Reay (2010), A novel weighting method for satellite magnetic data and a new global magnetic field model, *Geophysical Journal International*, 181, 250-260, doi: 10.1111/j.1365-246X.2010.04510.x.

Thomson, A. W. P. and V. Lesur (2007), An Improved Geomagnetic Data Selection Algorithm for Global Geomagnetic Field Modelling. *Geophysical Journal International*, 169, 951-963 doi: 10.1111/j.1365-246X.2007.03354.x.

Whaler, K. A., and C. D. Beggan (2015), Derivation and use of core surface flows for forecasting secular variation. *Journal of Geophysical Research: Solid Earth*, 120, 1400-1414, doi: 10.1002/2014JB011697.